



Chemiluminescence detection of kanamycin by DNA aptamer regulating peroxidase-like activity of Co_3O_4 nanoparticles

Xuxin Zhang¹ · Yihao Li¹ · Shaojie Xia¹ · Zhenyuan Yang¹ · Baiyun Zhang¹ · Yonghong Wang^{1,2}

Received: 6 August 2024 / Accepted: 9 September 2024
© The Author(s), under exclusive licence to The Japan Society for Analytical Chemistry 2024

Abstract

Kanamycin (KAN) is widely used as a growth hormone analog and an antibacterial agent. However, abuse of this substance has resulted in the accumulation of excessive residue levels in foods of animal origin, which presents a significant risk to human health. A chemiluminescent aptasensor was constructed for the rapid quantitative detection of KAN by combining the properties of Co_3O_4 nanoparticles (Co_3O_4 NPs) nanozyme activity and DNA aptamer with high specificity. The DNA aptamer/ Co_3O_4 NPs nanozyme regulated the chemiluminescence signal by exploiting the chemiluminescent properties of luminol oxidation by H_2O_2 . Specific binding of KAN to the aptamer led to the formation of a steric hindrance block in the solution, which inhibited the activity of nanozyme and reduced signal intensity. The degree of signal reduction is related to the concentration of KAN. Under optimal conditions, there was good linearity between KAN concentration and chemiluminescence signal intensity in the range of 0.5–8.0 μM , with a detection limit of 0.26 μM . The detection system performed well in the presence of competing antibiotics and was virtually unaffected. The method was also suitable for the detection of KAN in milk samples with sample recoveries of 97.8%–99.1%. The chemiluminescence sensor has the advantages of low cost, specificity, and sensitivity, and does not require an external light source or modification of the nucleic acid aptamer which makes it a promising candidate for applications in the field of food detection.

Keywords Chemiluminescence · Kanamycin · Peroxidase-like activity · Co_3O_4 NPs · Aptamer

Introduction

Kanamycin (KAN) is an important aminoglycoside antibiotic that could be widely used in veterinary medicine for the treatment of bacterial infections, it can also be used as a growth agent to accelerate the growth of livestock and poultry, and is currently widely used in the breeding industry of pigs, chickens, cattle and other animals [1, 2]. Excessive use of KAN leads to excessive residues of animal-derived food, causing serious harm to human health, such as hepatotoxicity, ototoxicity, myocardial inhibition, and even life-threatening [3]. Therefore, the effective determination of

trace amounts of KAN in animal-derived foods is of great significance [4]. To date, several methods have been used to analyze KAN in food or biological samples of animal origin, for instance, high-performance liquid chromatography (HPLC) [5, 6], capillary electrophoresis [7, 8], surface plasmon resonance (SPR) [9, 10] and enzyme-linked immunosorbent assay (ELISA) [11, 12]. Traditional detection methods can accurately quantify KAN but require sophisticated equipment, time-consuming procedures, or high reagent consumption, which limits their further application. Hence, there is still an extraordinary need for rapid, economical, and satisfactory methods for detecting KAN residues suitable for routine use [13, 14]. Chemiluminescence is an analytical method constructed by releasing the energy produced in the chemical reaction process through photons, it does not require an external light source and has been widely used by researchers because of its high sensitivity, fast response time, low detection limit, and easy to use [15]. The traditional chemiluminescence method has a low signal and weak luminescence, so an enhancer is needed to modulate the signal [16].

✉ Yonghong Wang
bionano@163.com

¹ Hunan Provincial Key Laboratory for Forestry Biotechnology and International Cooperation, Base of Science and Technology Innovation on Forest Resource Biotechnology, Central South University of Forestry and Technology, Changsha 410004, China

² Yuelushan Laboratory, Changsha 410004, China

Nanozymes are kind of nanomaterials with enzymatic activity, which have been widely used in bioassays due to their greater environmental tolerance than natural enzymes, and have attracted attention for their ability to emulate the chemical functionality of natural enzymes, as well as their superior stability and diverse applicability [17–19]. With the discovery of the activity of nanomaterial enzymes, metal-based nanozymes have been used as catalysts to regulate chemiluminescence signals [20–22]. For example, a chemiluminescent/photothermal dual-mode lateral flow immunoassay for gentamicin detection based on CoFe PBAs/WS₂ nanozyme was reported by Wu et al. [23]. Shi et al. [24] proposed a colorimetric sensor for phosphates discrimination and disease identification based on Cu₂Cl(OH)₃ nanozyme with conspicuous laccase and peroxidase-like activities. Shi's group [25] constructed a bimetallic nanozyme, which can synergize to regulate the behavior of oxygen intermediates and substrate 5-hydroxymethylfurfural adsorption. Although nanozymes can replace natural enzymes to perform enzyme-like activities, the lack of specific recognition elements limits their applications in the field of analysis [26].

Aptamer is a stretch of single-stranded DNA or RNA that binds specifically to a target molecule, including enzymes, antibodies, metal ions and biotoxins [27, 28]. Aptamer has been found to be a key factor affecting the catalytic activity of nanozymes. The catalytic reaction sites of nanozymes are located on their surfaces, and aptamers can be attached to them in various ways. Aptamer enables the nanozymes to uniquely recognize targets and thus modulate the catalytic activity of the nanozymes [29]. Therefore, aptamer-incorporating-nanozymes can be used to develop various aptamer sensors. In recent years, researchers have favored DNA aptamer, owing to its low cost, high specificity, stability, and wide range of target molecules [30–32]. DNA-nanozyme-based sensors have been reported to detect multiple targets and have greatly accelerated the development of nanozyme-based sensors [33].

Based on these considerations, we designed a platform for rapid quantitative detection of KAN. The DNA aptamer/Co₃O₄ NPs nanozyme regulated the chemiluminescence signal by oxidizing the chemiluminescence properties of luminol with H₂O₂. The steric hindrance block formed by the specific binding of KAN to the aptamer in solution would inhibit the activity of the nanozyme and thus decrease the signal intensity. The chemiluminescent sensor has the advantages of low cost, strong specificity, and high sensitivity, and does not require an external light source or modification of the nucleic acid aptamer, which has the potential for food safety applications.

Experimental section

Materials and reagents

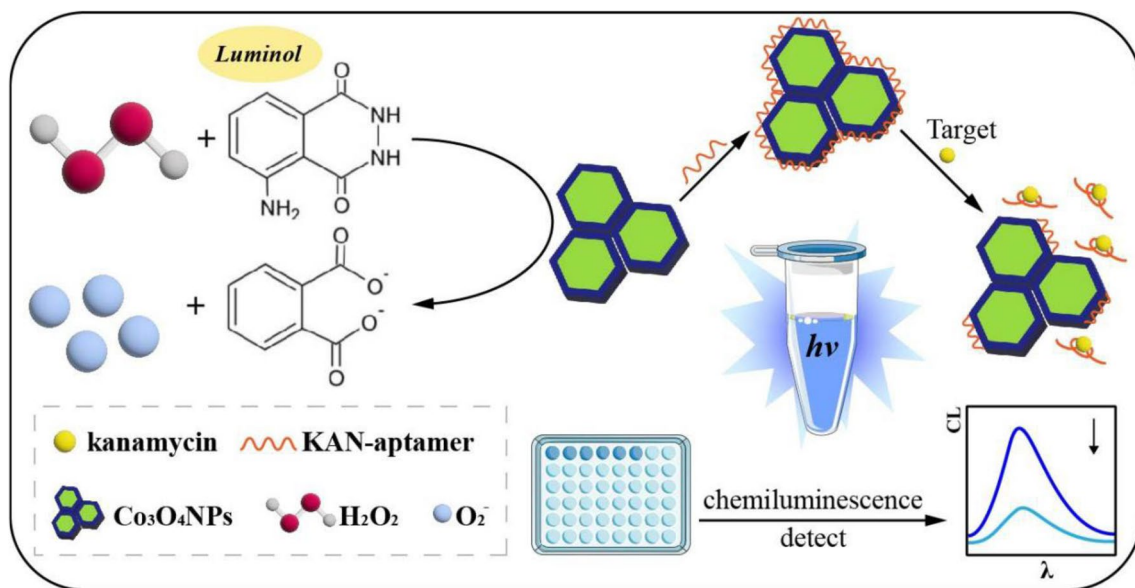
KAN aptamer [5'-TGGGGGTTGAGGCTAAGCCGA-3'] was synthesized and HPLC-purified by Sangon Biotechnology Co., Ltd. (Shanghai, China). The diluted DNA materials and raw DNA materials were stored in a -20 °C refrigerator. Cobalt acetate (Co(CH₃COO)₂·4H₂O) and ammonium were sourced from Sinopharm Chemical Reagent Co., Ltd. (Shanghai, China). Luminol used in the experiment was purchased from Phygene Life Sciences Co., Ltd. (Fujian, China). Acetic acid (HAc), KAN, tetracycline (TET), chlortetracycline (CTC), oxytetracycline (OTC), chloramphenicol (CPL), levofloxacin (LVFX), and sodium sulfadiazine (SD-Na) were purchased from Shanghai Aladdin Reagents Co., Ltd. (Shanghai, China). All pure water used in the experiment was purified by a Milli-Q ultrapure water instrument (Milli-Q™; Millipore, Burlington, MA, USA). A microplate reader with hybrid technology (BioTek, Winooski, VT, USA) was used to measure the chemiluminescence signal through the transparent 96-microwell plate purchased from Hunan Bkmam Biotechnology Co., Ltd. (Changsha, China).

Preparation of Co₃O₄ NPs

The required nanozymes were synthesized by hydrothermal method. Firstly, 1.0 g cobaltous acetate was added to 40.0 mL ultrapure water. After that, 2.5 mL of 25% ammonia was added to the beaker, and the solution was stirred until a uniform mixture was formed. The mixed solution was then transferred to a 50.0 mL reactor, sealed, and reacted at 180 °C for 12 h. After the reactor was cooled naturally, the black powder was collected and washed repeatedly with ultra-pure water to remove impurities. Finally, the black aqueous solution was dried at 60 °C for 4 h, and the obtained products were collected and used as nanozymes in subsequent experiments [34].

Feasibility experiments

It is necessary to determine whether an aptamer that binds specifically to KAN can modulate the catalytic activity of Co₃O₄ NPs. Co₃O₄ NPs was mixed with 5.0 μM KAN-apt solution in 2:1 volume to form a Co₃O₄ NPs/KAN-apt solution. In a transparent 96-microwell plate, wells A, B, and C were set up to represent three test systems with a total volume of 100.0 μL. Well A was the luminol-H₂O₂ system, well B represented the system with the addition



Scheme.1 Schematic diagram of the chemiluminescence for KAN detection based on Co_3O_4 NPs/KAN-apt

of the Co_3O_4 NPs/KAN-apt nanozymes based on well A, and well C represented the system with the addition of the substance to be detected to well B.

Wells A, B, and C contained 10.0 μL 2.0 mM H_2O_2 , 10.0 μL 500.0 μM luminol, and 30.0 μL buffer. An additional 30.0 μL of Co_3O_4 NPs/ Kan-apt solution was added to well B. Based on well B, an extra 20.0 μL KAN solution was added to well C. If the total volume of wells A, B, and C was less than 100.0 μL , ultra-pure water was supplemented. The chemiluminescence intensity at 300–600 nm was detected by microplate reader immediately after each sample addition. In addition, multiple parallel groups were set up for different systems to avoid test errors.

KAN detection by chemiluminescence

Firstly, Co_3O_4 NPs/KAN-apt was prepared in advance according to the preparation method described in Sect. “Feasibility experiments”. Subsequently, 20 μL of KAN at different concentrations were reacted with Co_3O_4 NPs/KAN-apt for optimal reaction time at room temperature, and 10 μL of the optimal concentration of H_2O_2 was added afterwards. Finally, 10 μL of the optimal concentration of luminol was added quickly, and the transparent 96-microwell plate was quickly placed into the microplate reader to record chemiluminescence spectroscopy. The results of the experiments were obtained from at least three repeated measurements. The linear range and lowest detection limit (LOD) of this chemiluminescence method for the detection of KAN were obtained from the spectrogram, and analyzed in comparison with other methods.

Recovery experiment of spiked sample

To validate the possibility of this sensor to detect KAN in real samples quantitatively, liquid milk was chosen as the spiked sample in the experiment. A simple pretreatment was performed on the milk samples: 20% acetic acid was added to 10.0 mL of milk samples until the pH of the solution reached 4.5, and the solution was centrifuged at 13,200 r/min for 15 min to remove the precipitate and obtain the supernatant, which was stored in a refrigerator at 4 $^\circ\text{C}$ [35]. KAN was added to the milk samples at concentrations of 1.0 μM , 2.0 μM , and 5.0 μM respectively. Test the spiked samples and calculate the recovery.

Results and discussion

Principle of the sensing assay

The whole process of the sensing scheme was exhibited in Scheme 1. In an alkaline environment, luminol was oxidized into an excited-state anion by the strong oxidizer H_2O_2 . When it returned to the ground state, energy was released in the form of photons, which microplate reader captured. Since the original state of KAN-apt was a one-dimensional linear ssDNA structure, Co_3O_4 NPs could immobilize KAN-apt on the surface by adsorption to form Co_3O_4 NPs/KAN-apt nanozymes, which catalyzed the generation of strong chemiluminescent signals from luminol- H_2O_2 . However, the presence of KAN would lead to a reduction in the signal. The reason for this phenomenon is that KAN-apt adsorbed

on the surface of Co_3O_4 NPs specifically bound with KAN in solution and desorbs from the surface of Co_3O_4 NPs, and the one-dimensional linear structure folds into a three-dimensional conformation, creating steric hindrance. Then, the steric effect led to a decrease in the number of luminol molecules and H_2O_2 molecules reaching the surface of the Co_3O_4 NPs/KAN-apt nanozymes, which in turn reduced the chemiluminescence signal. The specific binding of KAN to the aptamer modulated the peroxidase activity of Co_3O_4 NPs, and the chemiluminescence platform achieved quantitative detection through the change in signal, which lays a solid foundation for applying Co_3O_4 NPs in photometric detection.

Characterization of the prepared materials

Transmission electron microscopy (TEM) was used to investigate the ultrastructure of the synthesized materials.

Figure 1A and B indicated that these Co_3O_4 NPs were spherical and uniformly distributed, and the average diameter of Co_3O_4 NPs was estimated to be approximately 0.2 nm. The chemical state of elements in Co_3O_4 NPs was further verified by Energy dispersive spectrometer (EDS) and X-ray photoelectron spectroscopy (XPS). Figure 1C and D showed that only the coexistence of Co and O elements in the samples indicating that Co_3O_4 NPs with a spinel structure with high purity has been successfully prepared.

Feasibility analysis

As shown in Fig. 2A, the luminescence signal of luminol- H_2O_2 was very weak or absent in the absence of any catalyst (curve a). A strong chemiluminescent signal was present in the system of Co_3O_4 NPs/KAN-apt nanozymes (curve b), indicating that the synthesized Co_3O_4 NPs/KAN-apt nanozymes could act as signal enhancer by regulating the

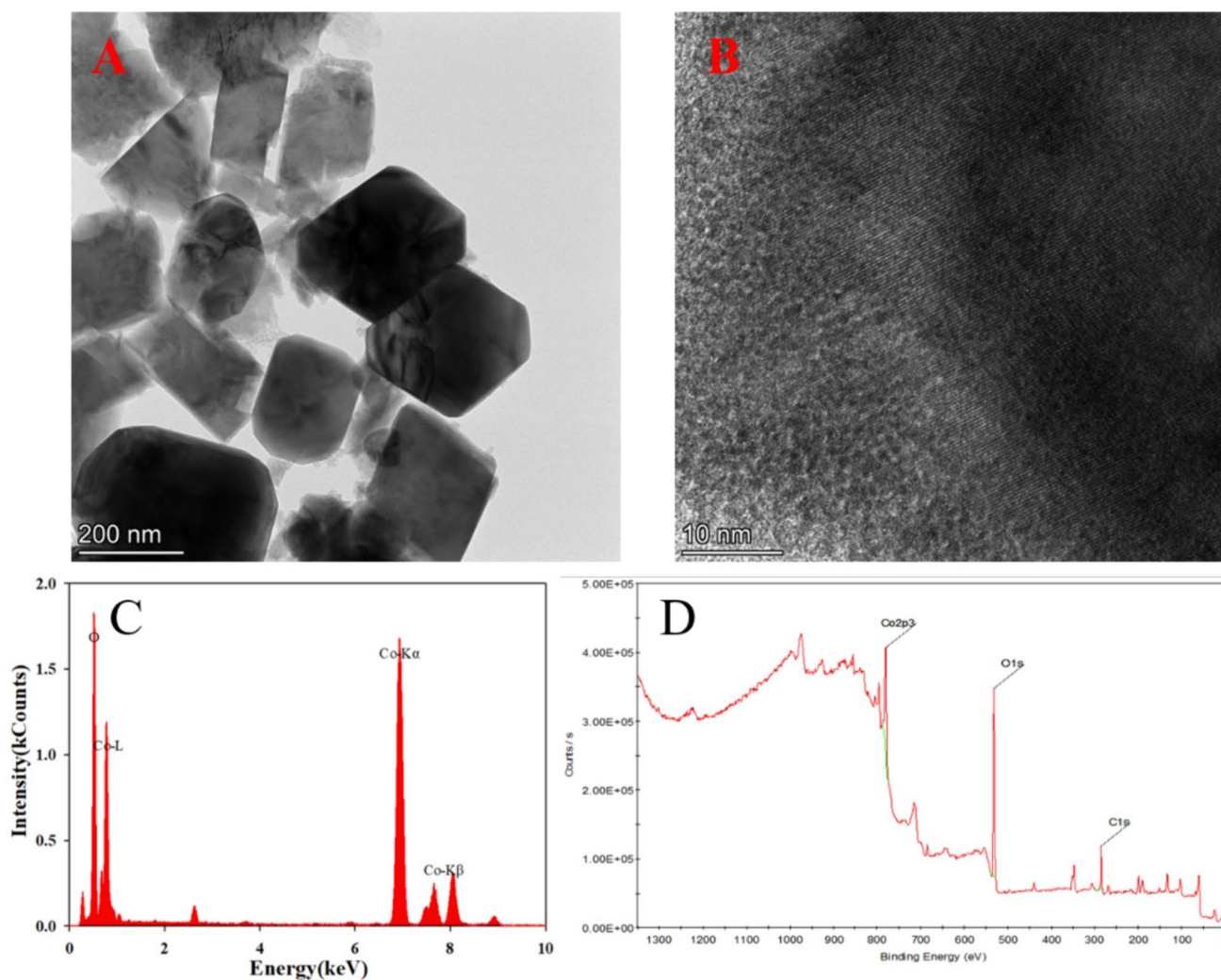


Fig. 1 **A** TEM of Co_3O_4 NPs (scale bar = 200 nm). **B** TEM of Co_3O_4 NPs (scale bar = 10 nm). **C** EDS of Co_3O_4 NPs. **D** XPS of Co_3O_4 NPs

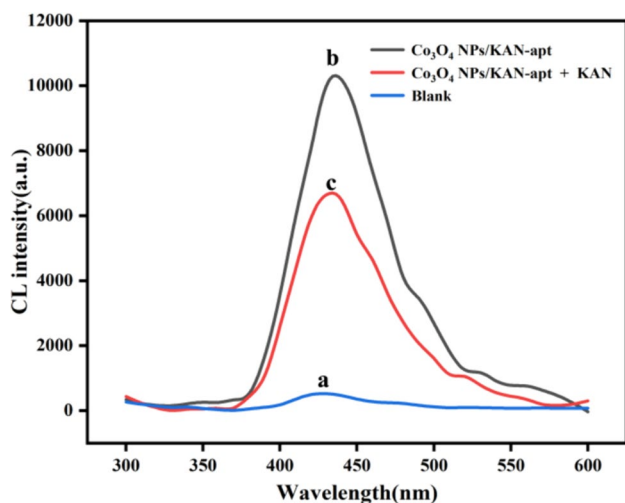


Fig. 2 Feasibility analysis diagram of chemiluminescence sensor. **a** luminol and H_2O_2 . **b** Co_3O_4 NPs, KAN-apt, luminol and H_2O_2 . **c** Co_3O_4 NPs, KAN-apt, KAN, luminol and H_2O_2

chemiluminescence signal of the luminol- H_2O_2 reaction and efficiently catalyzing the reaction of luminol- H_2O_2 . The signal was attenuated because the KAN would specifically bind with KAN-apt (curve c). Moreover, the only change in the reaction system was the addition of the target KAN, indicating that the signal change was only related to it. The results showed that the chemiluminescence sensor can indirectly measure the concentration of KAN through changes in the chemiluminescence signal.

Optimization of the experiment conditions

The detection process of KAN by the chemiluminescence method was affected by several factors. To optimize the detection performance of the sensor, experimental conditions were optimized, including the pH of the buffer, the concentration of luminol, and the concentration of H_2O_2 .

In Fig. 3A, we investigated the effect of the pH of the buffer on the response of the KAN aptasensor and utilized buffers of different pH values (11.0, 11.5, 12.0, 12.5, and 13.0). The results exhibited that the ΔCL signal first increased and then decreased with the increase in pH, and

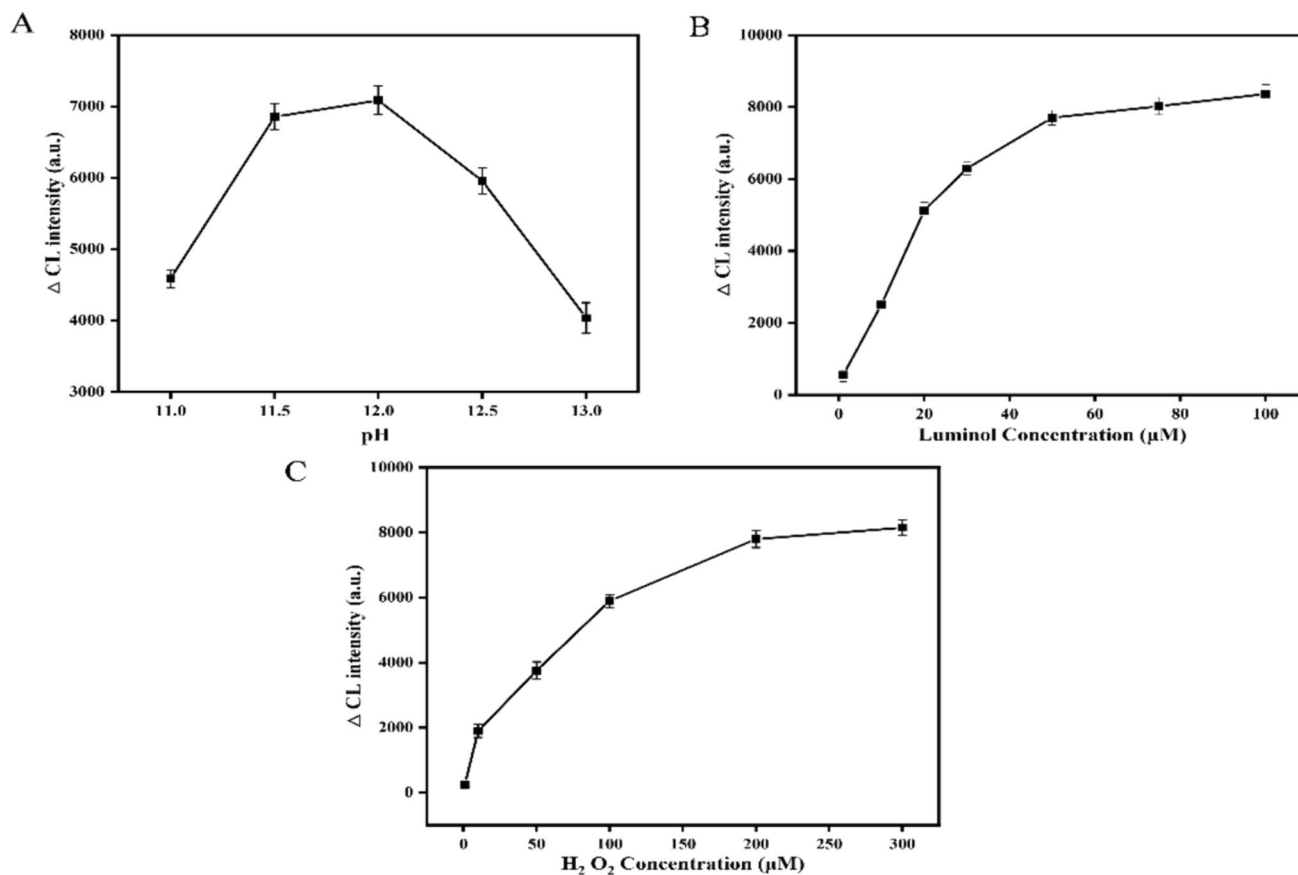


Fig. 3 Effect of different conditions on the chemiluminescent aptamer sensor. **A** pH (from left to right, 11.0, 11.5, 12.0, 12.5, 13.0, respectively); **B** concentration of luminol (from left to right, 1, 10, 20, 30,

50, 75, 100 μM , respectively); **C** concentration of H_2O_2 (from left to right, 1, 10, 50, 100, 200, 300 μM , respectively)

the signal reached a maximum when the pH of buffer was 12.0. When the pH of buffer exceeded 12.0, the upward trend turned downward. Therefore, the pH of 12.0 was chosen for this work.

The concentration of luminol also exerted a significant effect on the constructed system, and the effect of the concentration of luminol on the determination of KAN was investigated. A series of luminol concentrations from 1.0 μM to 100.0 μM was used as the research object. The results are shown in Fig. 3B, the ΔCL increased rapidly with increasing concentration from 1.0 μM to 50.0 μM , and the upward trend stabilized after 50.0 μM . Consequently, 50.0 μM was used as the optimal concentration for the experiment.

To determine the optimal condition, different concentrations of H_2O_2 were used in the experiments. As shown in Fig. 3C, the ΔCL signal increased significantly with increasing concentrations of H_2O_2 from 1.0 μM to 200.0 μM . The signal almost stabilized after 200.0 μM . Therefore, 200.0 μM was determined to be the optimal concentration of H_2O_2 for the next determination.

Performance of the system of KAN determination

In order to evaluate the performance of the constructed aptasensor, various concentrations of KAN were measured with this method. In ideal circumstances, these changes in the chemiluminescence intensity of the aptasensor were correlated with the concentration of KAN. A strong linear association was seen in Fig. 4 between the changes in CL and the logarithm values of KAN concentration in the range of 0.5–8.0 μM . The regression equation was $\Delta\text{CL} = 0.8960x + 299.9604$ with R^2 was 0.9960. The LOD of KAN was 0.26 μM . According to the results, the aptasensor has high sensitivity and low detection limit.

From Table 1, the manufactured aptasensor for the determination of KAN was compared with the previous studies. Compared to some methods for KAN detection, such as fluorescence assay and electrochemical assay, even though they have lower LOD and vast detection range, the sensor in this work is easy to operate, inexpensive, and has a shorter detection time. At the same time, the constructed sensor has lower LOD and higher stability compared with other rapid detection methods such as colorimetric assay and SPR. Therefore,

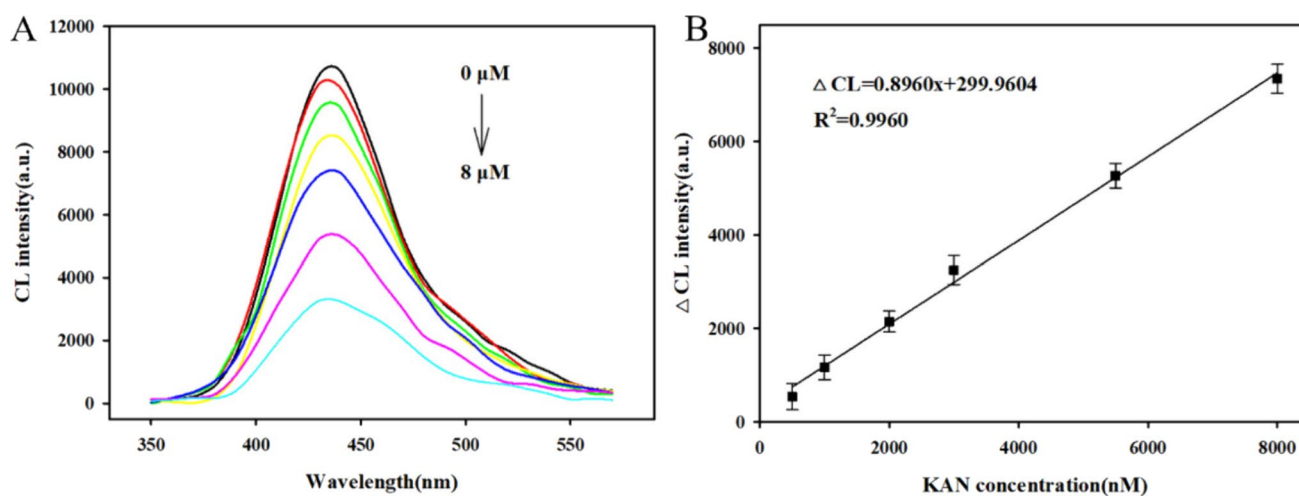


Fig. 4 **A** Chemiluminescence signal curves of KAN at different concentrations (0, 0.5, 1.0, 2.0, 3.0, 5.5, 8.0 μM) under optimal experimental conditions. **B** Linearity graph for the detection of KAN

Table 1 Comparison of the analytical performance of different methods for the detection of KAN

Technique	Limit of detection (nM)	Linear range (nM)	Recovery	Reference
Fluorescent assay	54	$54.0\text{--}9.0 \times 10^2$	96.89%–106.75%	[36]
Electrochemical assay	37	$1.0 \times 10^4\text{--}1.0 \times 10^6$	98.75%–108.28%	[37]
Colorimetric assay	628	$1.0 \times 10^2\text{--}1.0 \times 10^5$	99.97%–102.96%	[38]
Photothermal assay	410	$5.0 \times 10^2\text{--}5.0 \times 10^4$	92.2%–107.0%	[39]
Surface plasmon resonance method	280	$1.0 \times 10^3\text{--}1.0 \times 10^5$	94.53%–97.85%	[40]
Chemiluminescence	260	$5 \times 10^2\text{--}8.0 \times 10^3$	97.8%–99.1%	This work

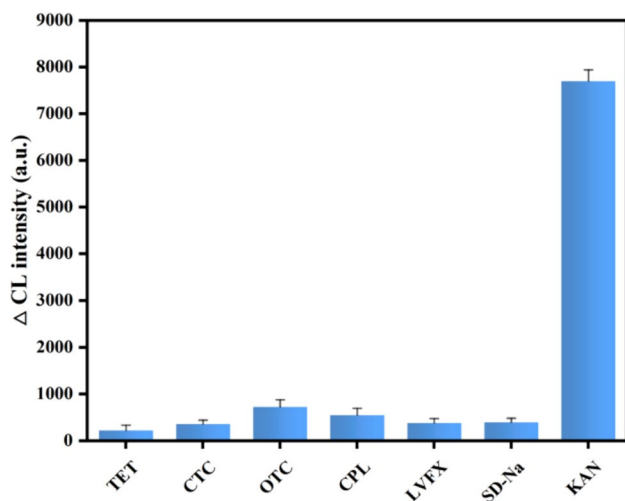


Fig. 5 Specificity of KAN detected by chemiluminescence

Table 2 Determination of KAN in fresh milk samples

Spiked KAN (mol/L)	Found KAN (mol/L)	Recovery (%)	RSD (%)
1.0×10^{-6}	9.91×10^{-7}	99.1	5.3
2.0×10^{-6}	1.97×10^{-6}	98.6	5.1
5.0×10^{-6}	4.89×10^{-6}	97.8	4.9

the manufactured aptasensor has the potential to be applied in the practical detection of KAN.

Specificity of the aptasensor

In order to evaluate the specificity of chemiluminescent sensors, several common antibiotics, such as TET, CTC, OTC, CPL, LVFX, and SD-Na, were selected as interfering factors to assess the effects on the sensor. Every antibiotic was incubated at a concentration of 8.0×10^{-6} mol/L. As can be shown in Fig. 5, the Δ CL increased more after being incubated with KAN solution than the other antibiotics, indicating that the constructed aptasensor that was exhibited exceptional selectivity.

Recovery in practical samples

Because the KAN has a tendency to remain in foods of animal origin, fresh milk was utilized as the test material to assess the practicality and viability of the aptasensor by detecting the recovery rate of different concentrations of KAN applied to the sample. As shown in Table 2, the addition of KAN exhibited a standard recovery rate ranging from 97.8% to 99.1%, with the relative standard deviation (RSD) below 5.3%. The results showed that the chemiluminescence

sensor is an accurate and reliable method for detecting KAN in real samples, providing data support for the application development of future products.

Conclusions

In this work, we constructed a chemiluminescent aptasensor for the detection of KAN by utilizing the activity of Co_3O_4 NPs/KAN-apt nanozyme to regulate the chemiluminescent signal of luminol- H_2O_2 , which owns the advantages of good sensitivity, high specificity, simplicity, and rapidity. The principle was based on the steric hindrance formed by KAN and KAN-apt, which decreased the chemiluminescence intensity and provided a basis for the determination of KAN. Under optimal conditions, the quantitative determination of KAN achieved a wide linear range from $0.5 \mu\text{M}$ to $8.0 \mu\text{M}$ and an excellent detection limit down to $0.26 \mu\text{M}$. Meantime, the sensor platform is highly specific for the detection of KAN and is not interfered with by competitive antibiotics. Hence, the proposed aptasensor can potentially be applied for KAN determination owing to the above-mentioned merits in food detection. Furthermore, the sensor has the ability to detect the corresponding aptamers according to the different targets, hence expanding the range of applications.

Acknowledgements This work was supported in part by the Hunan Provincial Natural Science Foundation of China (2024JJ8264), Training Program for Excellent Young Innovators of Changsha (kq2106053).

Authors contributions Xuxin Zhang: Investigation, Writing- Original draft preparation. Yihao Li: Original draft preparation. Shaojie Xia: Software, Validation. Zhenyuan Yang: Writing – review & editing, Formal analysis. Baiyun Zhang: Writing – review & editing. Yonghong Wang: Funding acquisition, Supervision.

Data availability All data generated or analyzed during this study are included in this article.

Declarations

Competing interest The authors declare that there is no conflict of interests regarding the publication of this article.

References

1. J.X. Li, M.Y. Luo, H.F. Yang, C. Ma, R. Cai, W.H. Tan, Novel dual-signal electrochemiluminescence aptasensor involving the resonance energy transform system for kanamycin detection. *Anal. Chem.* **94**, 6410–6416 (2022). <https://doi.org/10.1021/acs.analchem.2c01163>
2. W.C. Geng, H.M. Liu, Z.Y. Yan, J.Y. Ji, F. Wang, R.Y. Yang, A novel dual-model photoelectrochemical/electrochemical sensor based on Z-scheme TiO_2 disks/methylene blue for kanamycin detection. *Anal. Methods-uk.* **16**, 4691–4699 (2024). <https://doi.org/10.1039/d4ay01023j>

3. W.Y. Zou, J.J. Wang, S.Y. Yang, Y. Tang, X.J. Niu, Y.E. Wu, Porous-nanozyme-based colorimetric sensor for rapid detection of kanamycin in foods under neutral condition. *J. Food Sci.* **88**, 2009–2022 (2023). <https://doi.org/10.1111/1750-3841.16570>
4. Y.N. Jin, Y.Z. Zhang, H. Xu, X. Lu, Y.W. Yuan, W. Zhang, A ratiometric electrochemical aptasensor for sensitive detection of kanamycin in food based on entropy-driven strand displacement reaction. *Food Control* **161**, 110390 (2024). <https://doi.org/10.1016/j.foodcont.2024.110390>
5. X.P. Zhang, J.J. Wang, Q.H. Wu, L. Li, Y. Wang, H.L. Yang, Determination of kanamycin by high performance liquid chromatography. *Molecules* **24**, 1902 (2019). <https://doi.org/10.3390/molecules24101902>
6. H. Hamidi, M. Zarrineh, A. Es-haghi, A. Ghasempour, Rapid and sensitive determination of neomycin and kanamycin in measles, mumps, and rubella vaccine via high-performance liquid chromatography–tandem mass spectrometry using modified superparamagnetic Fe₃O₄ nanospheres. *J. Chromatogr. A* **1625**, 461343 (2020). <https://doi.org/10.1016/j.chroma.2020.461343>
7. Y.F. Lin, Y.C. Wang, Y.S. Chang, Capillary electrophoresis of aminoglycosides with argon-ion laser-induced fluorescence detection. *J. Chromatogr. A* **1188**, 331–333 (2008). <https://doi.org/10.1016/j.chroma.2008.01.088>
8. C.Z. Yu, Y.Z. He, G.N. Fu, H.Y. Xie, W.E. Gan, Determination of kanamycin A, amikacin and tobramycin residues in milk by capillary zone electrophoresis with post-column derivatization and laser-induced fluorescence detection. *J. Chromatogr. B* **877**, 333–338 (2009). <https://doi.org/10.1016/j.jchromb.2008.12.011>
9. D.F. Feng, X.C. Tan, Y.Y. Wu, C.H. Ai, Y.N. Luo, Q.Y. Chen, H.Y. Han, Electrochemiluminescence nanogears aptasensor based on MIL-53(Fe)@CdS for multiplexed detection of kanamycin and neomycin. *Biosens. Bioelectron.* **129**, 100–106 (2019). <https://doi.org/10.1016/j.bios.2018.12.050>
10. X.M. Wang, C. Chen, G.I.N. Waterhouse, X.G. Qiao, Z.X. Xu, A novel SERS sensor for the ultrasensitive detection of kanamycin based on a Zn-doped carbon quantum dot catalytic switch controlled by nucleic acid aptamer and size-controlled gold nanorods. *Food Chem.* **362**, 130261 (2021). <https://doi.org/10.1016/j.foodchem.2021.130261>
11. P. Su, X.N. Chen, Z.J. He, Y. Yang, Preparation of polyclonal antibody and development of a biotin-streptavidin-based ELISA method for detecting kanamycin in milk and honey. *Chem. Res. Chinese U.* **33**, 876–881 (2017). <https://doi.org/10.1007/s40242-017-7168-9>
12. L. Jiang, D.L. Wei, K. Zeng, J. Shao, F. Zhu, D.L. Du, An enhanced direct competitive immunoassay for the detection of kanamycin and tobramycin in milk using multienzyme-particle amplification. *Food Anal. Method.* **11**, 2066–2075 (2018). <https://doi.org/10.1007/s12161-018-1185-2>
13. L. Zheng, Q. Li, X.K. Deng, Q.F. Guo, D.D. Liu, G.M. Nie, A novel electrochemiluminescence biosensor based on Ru(bpy)₃²⁺-functionalized MOF composites and cycle amplification technology of DNAzyme walker for ultrasensitive detection of kanamycin. *J. Colloid Interf. Sci.* **659**, 859–867 (2024). <https://doi.org/10.1016/j.jcis.2024.01.045>
14. X.J. Wang, X.Y. Yuwen, S.S. Lai, X. Li, G.S. Lai, Enhancement of telomerase extension via quadruple nucleic acid recycling to develop a novel colorimetric biosensing method for kanamycin assay. *Anal. Chim. Acta* **1287**, 342139 (2024). <https://doi.org/10.1016/j.aca.2023.342139>
15. L.Y. Yu, X.Q. Zhang, D.B. Jin, F.X. Lou, J.K. Zhao, X. Hun, Chemiluminescence assay for kanamycin based on target recycling strategy. *Luminescence* **37**, 987–994 (2022). <https://doi.org/10.1002/bio.4250>
16. S.T. Cheng, H.M. Liu, H. Zhang, G.L. Chu, Y.M. Guo, X. Sun, Ultrasensitive electrochemiluminescence aptasensor for kanamycin detection based on silver nanoparticle-catalyzed chemiluminescent reaction between luminol and hydrogen peroxide. *Sensor Actuat. B Chem.* **304**, 127367 (2020). <https://doi.org/10.1016/j.snb.2019.127367>
17. M.E. Zheng, M.X. Liu, Z.C. Song, F. Ma, H.D. Zhu, H.L. Guo, H.M. Sun, High-precision colorimetric-fluorescent dual-mode biosensor for detecting acetylcholinesterase based on a trimetallic nanozyme for efficient peroxidase-mimicking. *J. Mater. Sci. Technol.* **191**, 168–180 (2024). <https://doi.org/10.1016/j.jmst.2024.01.013>
18. Q. Quan, J.J. Tong, L.F. Chen, S.Y. Fang, M.J. Li, L.L. Wu, Z.H. Qin, Freezing-directed construction of enzyme/nano interfaces: Reagentless conjugation, superior activity, and better stability. **35**, 108894 (2024). <https://doi.org/10.1016/j.ccllet.2023.108894>
19. K. Quan, X.Y. Li, J.Q. Deng, W.J. Chen, Z. Zou, K. Chen, L.L. Wu, J.W. Liu, Z.H. Qin, Pt-decorated gold nanoflakes for high-fidelity phototheranostics: reducing side-effects and enhancing cytotoxicity toward target cells. *Angew. Chem. Int. Edit.* **63**, 20 (2024). <https://doi.org/10.1002/anie.202402881>
20. J.Y. Zhang, J.W. Liu, Nanozyme-based luminescence detection. *Luminescence* **35**, 1185–1194 (2020). <https://doi.org/10.1002/bio.3893>
21. J. Qin, N.N. Guo, J. Yang, J. Wei, Recent advances in metal oxide nanozyme-based optical biosensors for food safety assays. *Food Chem.* **447**, 139019 (2024). <https://doi.org/10.1016/j.foodchem.2024.139019>
22. S. Payal, A. Krishnamoorthy, J.A. Elumalai, C. Moses, Anandharamakrishnan, A review on recent developments and applications of nanozymes in food safety and quality analysis. *Food Anal. Method.* **14**, 1537–1558 (2021). <https://doi.org/10.1007/s12161-021-01983-9>
23. L.L. Wu, Z.J. Zhu, J.X. Xue, L. Zheng, H.M. Liu, H. Ouyang, Z.F. Fu, Y. He, Chemiluminescent/photothermal dual-mode lateral flow immunoassay based on CoFe PBAs/WS₂ nanozyme for rapid and highly sensitive point-of-care testing of gentamicin. *Biosens. Bioelectron.* **265**, 116711 (2024). <https://doi.org/10.1016/j.bios.2024.116711>
24. Q.H. Shi, Y. Wang, Q.F. Zhang, Y.J. Dai, F.F. Liu, W.J. Jing, Cu₂Cl(OH)₃ nanozyme-based colorimetric sensor array for phosphates discrimination and disease identification. *Talanta* **280**, 26724 (2024). <https://doi.org/10.1016/j.talanta.2024.126724>
25. L. Shi, Q. Li, S. Liu, X.Y. Liu, S.C. Yang, C.X. Chen, Z.J. Li, S. Liu, Bimetallic nanozymes synergize to regulate the behavior of oxygen intermediates and substrate HMF adsorption. *Chem. Commun.* **60**, 8860–8863 (2024). <https://doi.org/10.1039/d4cc03213f>
26. Y.C. Li, Q.Y. Bao, Z.Q. Wang, Y.J. Huang, D.H. Zhang, Y.Z. Shen, J. Cheng, J.L. Wang, Artificial enzyme mimics cascade catalysis for signal amplification and transduction in food quality determination: An overview of fundamentals and recent advances. *Coordination Chem. Rev.* **505**, 215689 (2024). <https://doi.org/10.1016/j.ccr.2024.215689>
27. K.M. Song, M. Cho, H. Jo, K. Min, S.H. Jeon, T. Kim, M.S. Han, J.K. Ku, C. Ban, Gold nanoparticle-based colorimetric detection of kanamycin using a DNA aptamer. *Anal. Biochem.* **415**, 175–181 (2011). <https://doi.org/10.1016/j.ab.2011.04.007>
28. T.K. Sharma, J.G. Bruno, A. Dhiman, ABCs of DNA aptamer and related assay development. *Biotechnol. Adv.* **35**, 275–301 (2017). <https://doi.org/10.1016/j.biotechadv.2017.01.003>
29. T.K. Sharma, R. Ramanathan, P. Weerathunge, M. Mohammadtazeri, H.K. Daima, R. Shukla, V. Bansal, Aptamer-mediated ‘turn-off/turn-on’ nanozyme activity of gold nanoparticles for kanamycin detection. *Chem. Commun.* **50**, 15856–15859 (2014). <https://doi.org/10.1039/c4cc07275h>
30. J.Q. Deng, J.Y. Xu, M.Z. Ouyang, Z. Zou, Y.L. Lei, J.B. Li, Z.H. Qin, R.H. Yang, Target-triggered hairpin-free chain-branching growth of DNA dendrimers for contrast-enhanced imaging in

- living cells by avoiding signal dispersion. *Chinese Chem. Lett.* **33**, 773–777 (2022). <https://doi.org/10.1016/j.ccllet.2021.08.046>
31. H.L. Yang, L. Xia, L.T. Li, Y. Tang, L.H. Huang, H. Tao, Y.E. Wu, Design an aptamer-recognized visual nanozyme sheet for rapid detection of ethyl carbamate in liquor. *J. Food Compos. Anal.* **128**, 106077 (2024). <https://doi.org/10.1016/j.jfca.2024.106077>
 32. Y.L. Lei, C.C. Li, X.Y. Ji, H.Y. Sun, X.W. Liu, Z.H. Mao, W.J. Chen, Z.H. Qin, J.W. Liu, Lowering entropic barriers in triplex DNA switches facilitating biomedical applications at physiological pH. *Angew. Chem. Int. Edit.* **63**, 19 (2024). <https://doi.org/10.1002/anie.202402123>
 33. R.Z. Yu, R. Wang, Z.Y. Wang, Q.S. Zhu, Z.H. Dai, Applications of DNA-nanozyme-based sensors. *Analyst* **146**, 1127–1141 (2021). <https://doi.org/10.1039/d0an02368j>
 34. Y.M. Dong, K. He, L. Yin, A.M. Zhang, A facile route to controlled synthesis of Co₃O₄ nanoparticles and their environmental catalytic properties. *Nanotechnology* **18**, 435602–435608 (2007). <https://doi.org/10.1088/0957-4484/18/43/435602>
 35. C.K. Wang, D. Chen, Q.Q. Wang, R. Tan, Kanamycin detection based on the catalytic ability enhancement of gold nanoparticles. *Biosens. Bioelectron.* **91**, 262–267 (2017). <https://doi.org/10.1016/j.bios.2016.12.042>
 36. Y.Y.C. Bao, Y.D. Sang, X.M. Yan, M.Y. Hu, N. Wang, Y.F. Dong, L.H. Wang, A enzyme-free fluorescence quenching sensor for amplified detection of kanamycin in milk based on competitive triggering strategies. *Rsc Adv.* **14**, 19076–19082 (2024). <https://doi.org/10.1039/d4ra01703j>
 37. M. Yin, L. Zhang, X.X. Wei, Y.W. Sun, S.Y. Qi, Y. Chen, X.X. Tian, J.X. Qiu, D.P. Xu, Spongy Co/Ni-Bio-MOF-based electrochemical aptasensor for detection of kanamycin based on coral-like ZrO₂@Au as an amplification platform. *J. Electroanal. Chem.* **920**, 116647 (2022). <https://doi.org/10.1016/j.jelechem.2022.116647>
 38. J.J. Lu, X.X. Xu, J. Chen, Polyoxometalate-based nanozyme with laccase-mimicking activity for kanamycin detection based on colorimetric assay. *Microchim. Acta* **191**, 544 (2024). <https://doi.org/10.1007/s00604-024-06621-9>
 39. H.B. Lee, S.E. Son, C.H. Ha, D. Kim, G.H. Seong, Dual-mode colorimetric and photothermal aptasensor for detection of kanamycin using flocculent platinum nanoparticles. *Biosens. Bioelectron.* **249**, 116007 (2024). <https://doi.org/10.1016/j.bios.2024.116007>
 40. E.M. Écija-Arenas, T. Kirchner, J.M. Hirsch, Fernández-Romero, Development of an aptamer-based SPR-biosensor for the determination of kanamycin residues in foods. *Anal. Chim. Acta* **1169**, 338631 (2021). <https://doi.org/10.1016/j.aca.2021.338631>

Springer Nature or its licensor (e.g. a society or other partner) holds exclusive rights to this article under a publishing agreement with the author(s) or other rightsholder(s); author self-archiving of the accepted manuscript version of this article is solely governed by the terms of such publishing agreement and applicable law.